



Research article

Modelling landscape dynamics with LST in protected areas of Western Ghats, Karnataka

T.V. Ramachandra ^{a, b, c, *, 1}, Setturu Bharath ^{a, 1}, Nimish Gupta ^{a, 1}^a Energy & Wetlands Research Group, Centre for Ecological Sciences (CES), Indian Institute of Science, Bangalore, Karnataka, India^b Centre for Sustainable Technologies (astra), Indian Institute of Science, Bangalore, Karnataka, India^c Centre for Infrastructure, Sustainable Transportation and Urban Planning (CISTUP), Indian Institute of Science, Bangalore, Karnataka, India

ARTICLE INFO

Article history:

Received 11 May 2017

Received in revised form

25 July 2017

Accepted 1 August 2017

Available online xxx

Keywords:

Forests

Hydrology

LULC dynamics

CA-Markov

Sustainable management

ABSTRACT

Forest ecosystems sustain biota on the earth as they are habitat to diverse biotic species, arrests soil erosion, play a crucial role in water cycle, sequester carbon, and helps in mitigating the impacts of global warming. Large scale land use land cover (LULC) change leading to deforestation is one of the drivers of global climate changes and alteration of biogeochemical cycles with significant consequences in ecosystem services and biodiversity. This has necessitated the investigation of LULC by mapping, monitoring and modelling spatio-temporal patterns and evaluating these in the context of human-environment interactions. The current work investigates LULC changes with temperature dynamics of select protected areas in Western Ghats. The land use analyses reveal changes in the forest cover across Kudremukh National Park (KNP), Rajiv Gandhi Tiger Reserve (RTR), Bandipur Tiger Reserve (BTR). KNP region has lost evergreen forest cover during 1973–2016 from 33.46 to 27.22%, while BTR lost deciduous cover from 61.69 to 47.3% due to mining, horticulture plantations, human habitations, etc. The LST increase has impacted regeneration of species with the induced water stress, etc. CA-Markov modelling was used for forecasting the likely land uses in 2026 and validation was done through Kappa indices. Results highlight decline of evergreen cover in KNP (9%) and deciduous cover in RTR (2%) followed by BTR (3%) with further expansion of plantations, which will impact biodiversity, hydrology and ecology. Insights of LULC dynamics help natural resource managers in evolving appropriate strategies to ensure conservation of threatened biota in Western Ghats.

© 2017 Elsevier Ltd. All rights reserved.

1. Introduction

Forest landscapes with diverse life forms are complex interactive ecosystems that support economy evident from the estimate of 4.7 trillion dollars annually through goods and services from global forest ecosystems (Krieger, 2001; de Groot et al., 2012). Unplanned developmental activities have led to the destruction of pristine forests and grasslands at regional as well as global scales (Lambin and Meyfroidt, 2011) evident from barren hilltops, reduced duration of stream flow, etc. Anthropogenic forces have modified over 83% of the Earth's land cover threatening sustenance of biological diversity (Sanderson et al., 2002 Fischer and Lindenmayer, 2007).

The conversion of natural ecosystems is the second largest driver of human-induced climate change, which accounts for 10% of anthropogenic carbon dioxide (CO₂) emissions (Le Quéré et al., 2013). Changes in forested landscape alter composition and configuration, affecting respective ecosystem functions. Fig. 1 illustrates various drivers of landscape degradation and its role in climate change. LULC change alters the homogeneous landscape into a mosaic of heterogeneous patches, which leads to the habitat fragmentation with smaller and more isolated patches (Ramachandra et al., 2016a). Consequences are reduction in natural resources availability (Vinay et al., 2013), biodiversity (Hansen et al., 2004), and changes in local climate (Chase et al., 2000; Bharath et al., 2013; Ramachandra 2014) as well as to global climate (Bagley et al., 2014; Val Martin et al., 2015; Halder et al., 2016). This emphasizes the need for conservation of forests to mitigate changes in the climate and to sustain water and food.

Protected areas (PA), national parks (NP), sanctuaries, nature reserves, wildlife refuges, wilderness areas have been created

* Corresponding author. Energy & Wetlands Research Group, CES TE15, Centre for Ecological Sciences, Indian Institute of Science, Bangalore, 560019, India.

E-mail address: cestvr@ces.iisc.ernet.in (T.V. Ramachandra).

¹ Web URL: <http://ces.iisc.ernet.in/energy>; <http://ces.iisc.ernet.in/foss>.

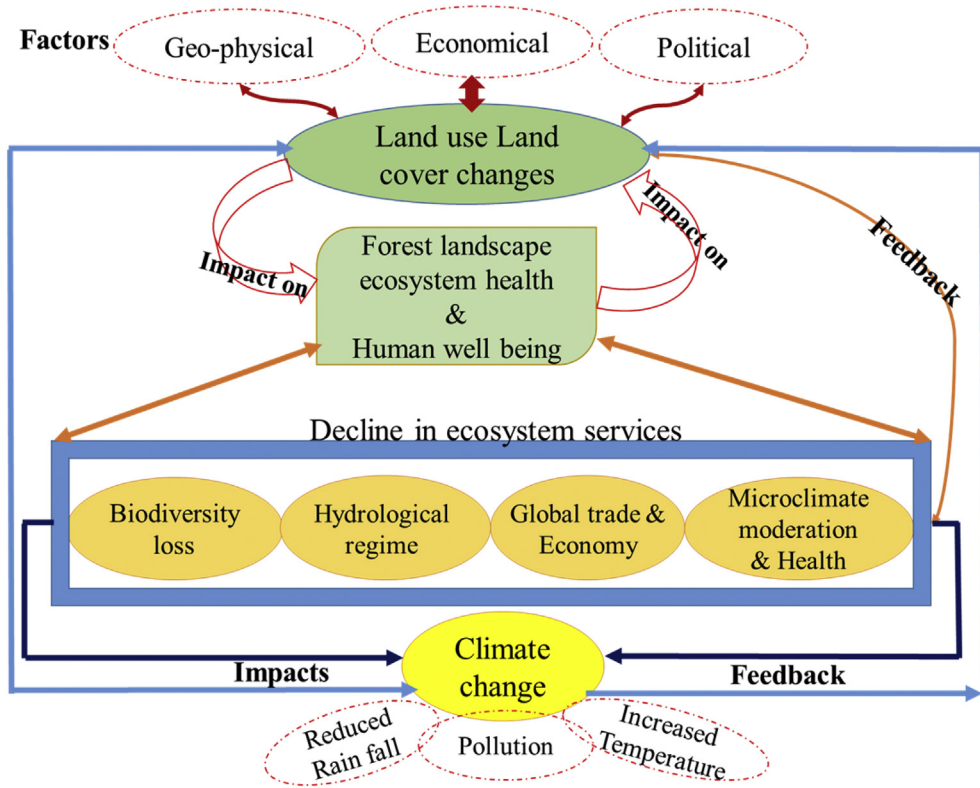


Fig. 1. Consequences of LULC changes.

through policy initiatives in order to protect the native habitat of endemic species and to reduce the magnitude of land conversion. Thus, PA system has evolved strategically to protect and maintain biological diversity, cultural resources at local to global scales. Maintaining ecological integrity in the protected area with buffer region is essential as most of protected landscapes are open systems that face anthropogenic and other biotic threats from adjacent areas. Alterations in landscape structure with a reduction in contiguous forests would increase the likelihood of invasive plants and animal range expansions, alter hydrologic regime (water availability), which leads to the erosion of integrity of the protected ecosystems. These are supposed to be managed through legal or other effective means from extinction especially those on the brink of extinction (Gaston et al., 2008). Globally, establishing PAs has gained impetus for conservation and according to the International Union for the Conservation of Nature (IUCN), nearly 13% of the global land surface is now under some form of protection. Land use land cover (LULC) mapping and monitoring of PAs can serve as important indicators of landscape and environmental status, distributions, and patterns. PA networks, conservation reserves, sanctuaries are created under various policy initiatives (Wild Life (Protection) Act 1972, Forest Conservation Act 1980, Environment (Protection) Act 1986, Biodiversity Act 2002) in order to conserve the forests from unregulated exploitation. The landscape surrounding protected areas also known as buffer region, influences PA's ability to maintain ecosystem functions and achieve conservation goals. The health of any PAs indirectly depends on surrounding buffer regions (Kintz et al., 2006). Drastic LU changes in buffer regions around PAs can reduce their effective size and limit their ability to conserve biodiversity because of alterations in ecological processes and the ability of organisms to move freely among protected areas (Hamilton et al., 2013). LULC changes in buffer zones surrounding protected ecological reserves will have

serious implications in the management and conservation of protected areas.

LULC changes involving conversion of land with vegetation cover to other land uses (built up, agriculture, barren land) have also increased land surface temperature (LST) (Mallick et al., 2008; Pal and Ziaul, 2016) due to alterations in the degree of absorption, surface temperature, evaporation rates, storage of heat, energy and water balance processes (Li et al., 2016). LULC induced LST changes play a vital role in many environmental processes affecting microclimate through associated biophysical changes (D'Odorico et al., 2013; Bharath et al., 2013). Moreover, warming aggravates tree mortality, regeneration of species with the induced water stress, which would further reduce forest cover (Allen et al., 2015). Vegetation die-off will rapidly alter ecosystem nature and properties at a regional scale. Thus, it is essential to monitor LULC changes to mitigate the impacts of changes in climate at a global scale. Multi-resolution (spatial, spectral, radiometric and temporal) remote sensing (RS) data with Geographical Information System (GIS) and modelling techniques provided a precise evaluation of the spread and health of forest ecosystem and forecasting. Accurate up to date LULC change information helps in addressing environmental consequences, protecting natural resources and planning (Ramachandra et al., 2016b). Modelling and visualization is considered as a conceptual, mathematical approach to account driving forces of change in a landscape such as socioeconomic, political, natural and cultural factors (Verburg et al., 2004; Batty and Torrens, 2005; Ramachandra et al., 2014). Cellular automata (CA), Markov chain models, and agent-based modelling approaches have been implemented for comprehensive projection of a region (Matthews et al., 2007; Bharath et al., 2014). Since forest land use changes are non-linear process, CA-Markov LULC models are efficient in prediction compared to the traditional mathematical models for decision making and planning (Mondal et al., 2016). It is

simple and provides a better understanding of how nonlinear process can aptly be simulated with less complexity (Pontius and Malanson, 2005; Grinblat et al., 2016). CA-Markov modelling technique exhibits better capabilities of descriptive power and simple trend projection of spatial changes as compared to other techniques (Chen et al., 2013). Objectives of the study are

- (i) to analyze current status and trends in temporal LULC patterns of forest cover in and around select PAs of central Western Ghats (Karnataka) from 1973 to 2016,
- (ii) assessment of temporal variations in temperature with change in LULC,
- (iii) modelling and visualization of spatial patterns of forests in 2026.

2. Materials and method

2.1. Study area

The Western Ghats is one among the 35 global hotspots of biodiversity and it lies in the western part of peninsular India in a series of hills stretching over a distance of 1600 km from north to south and covering an area of about 1,60,000 sq.km. It harbors very rich flora and fauna and there are records of over 4600 species of flowering plants with 38% endemics, 330 butterflies with 11% endemics, 197 reptiles with 52% endemics, 529 birds with 5% endemics, 161 mammals with 12% endemics, 343 fishes with 39% endemics and 248 amphibians with 62% endemics (<http://wgbsi.ces.iisc.ernet.in/biodiversity/>). Unplanned developmental activities during the post-industrialization period have threatened biodiversity, ecology and water availability. In this context, the government of India has created PAs network across wild habitats in order to conserve and reduce impacts. Fig. 2 depicts the locations of Kudremukh National Park (KNP), Rajiv Gandhi Tiger Reserve (RTR), Bandipur Tiger Reserve (BTR), which were chosen to understand the status of forests and LU dynamics. KNP comes under the Global Tiger Conservation Priority-I (as per Wildlife Conservation Society (WCS) and World Wide Fund-USA) and is a habitat to diverse endemic tax. RTR is also known as Nagarhole National Park, sensitive habitat to elephants (connects to Nilgiri Biosphere Reserve), and has been experiencing anthropogenic pressure, evident from degradation of forests, intensified agricultural activities. BTR is the first NP to get status as tiger reserve (TR) in 1973, which is also a habitat for numerous bird species (~250 species) and mammals endemic to Western Ghats. Rampant habitat degradations are common phenomenon across PAs due to unplanned developmental projects such as dams and interstate highways in the ecologically sensitive habitats apart from other pressures such as grazing, firewood collection and weed infestation (*Eupatorium*, *Parthenium*, *Chromolaena odorata*), illegal hunting, poaching (elephant poaching for ivory), etc. due to lack of effective eco-management leading to a very frequent instances of human-animal conflicts. Unauthorized occupation of forest lands for cultivation in the buffer region has aggravated human-animal conflicts leading to the frequent animal mortalities.

(RTR), Bandipur Tiger Reserve (BTR), which were chosen to understand the status of forests and LU dynamics. KNP comes under the Global Tiger Conservation Priority-I (as per Wildlife Conservation Society (WCS) and World Wide Fund-USA) and is a habitat to diverse endemic tax. RTR is also known as Nagarhole National Park, sensitive habitat to elephants (connects to Nilgiri Biosphere Reserve), and has been experiencing anthropogenic pressure, evident from degradation of forests, intensified agricultural activities. BTR is the first NP to get status as tiger reserve (TR) in 1973, which is also a habitat for numerous bird species (~250 species) and mammals endemic to Western Ghats. Rampant habitat degradations are common phenomenon across PAs due to unplanned developmental projects such as dams and interstate highways in the ecologically sensitive habitats apart from other pressures such as grazing, firewood collection and weed infestation (*Eupatorium*, *Parthenium*, *Chromolaena odorata*), illegal hunting, poaching (elephant poaching for ivory), etc. due to lack of effective eco-management leading to a very frequent instances of human-animal conflicts. Unauthorized occupation of forest lands for cultivation in the buffer region has aggravated human-animal conflicts leading to the frequent animal mortalities.

2.2. Method

Mapping, monitoring, modelling and visualization of LULC dynamics in the select protected areas with 10 km buffer in the central Western Ghats has been carried out as discussed in Fig. 3. Remote sensing (RS) data used in the study are Landsat MSS (1973), TM (1992), OLI8 (2016), IRS p6L4X (2016), and online Google Earth data (<http://earth.google.com>). Topographic maps have provided ground control points to rectify RS data and scanned paper maps. Survey of India (SOI) toposheets (1:50000 and 1:250000 scales) and vegetation map of South India developed by French Institute (1986) of scale 1:250000 was digitized to identify various forest cover types and temporal analyses to find out the changes in

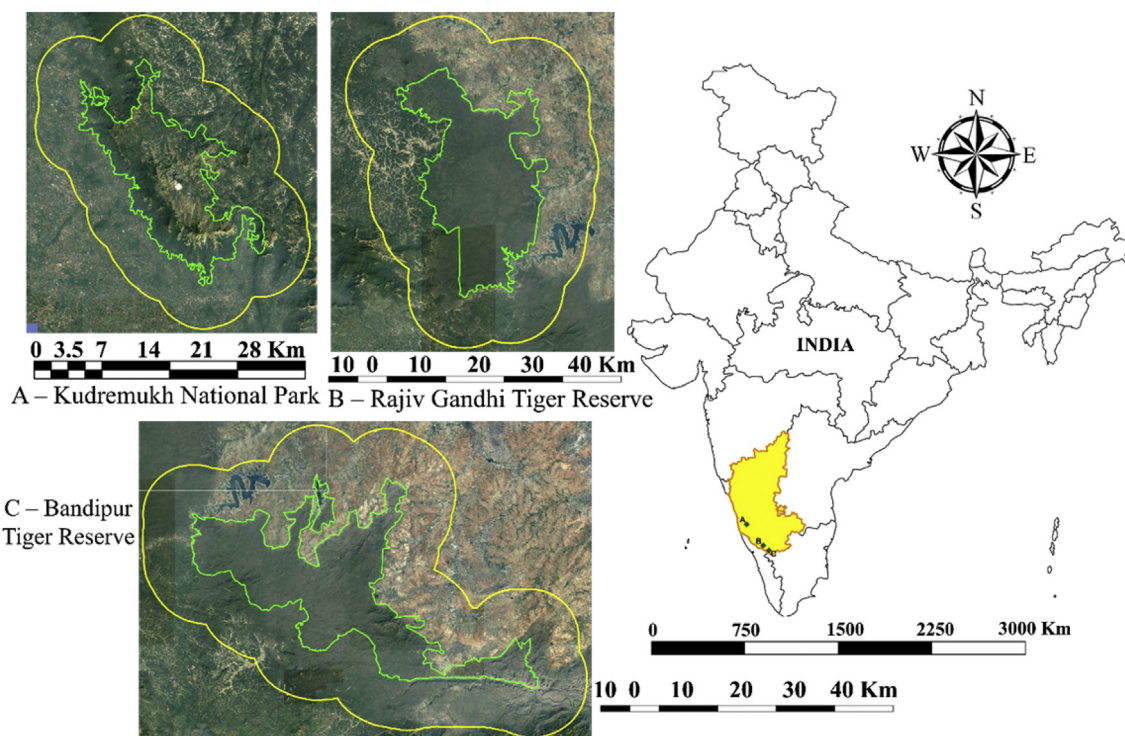


Fig. 2. Study area - select protected areas of Western Ghats, Karnataka.

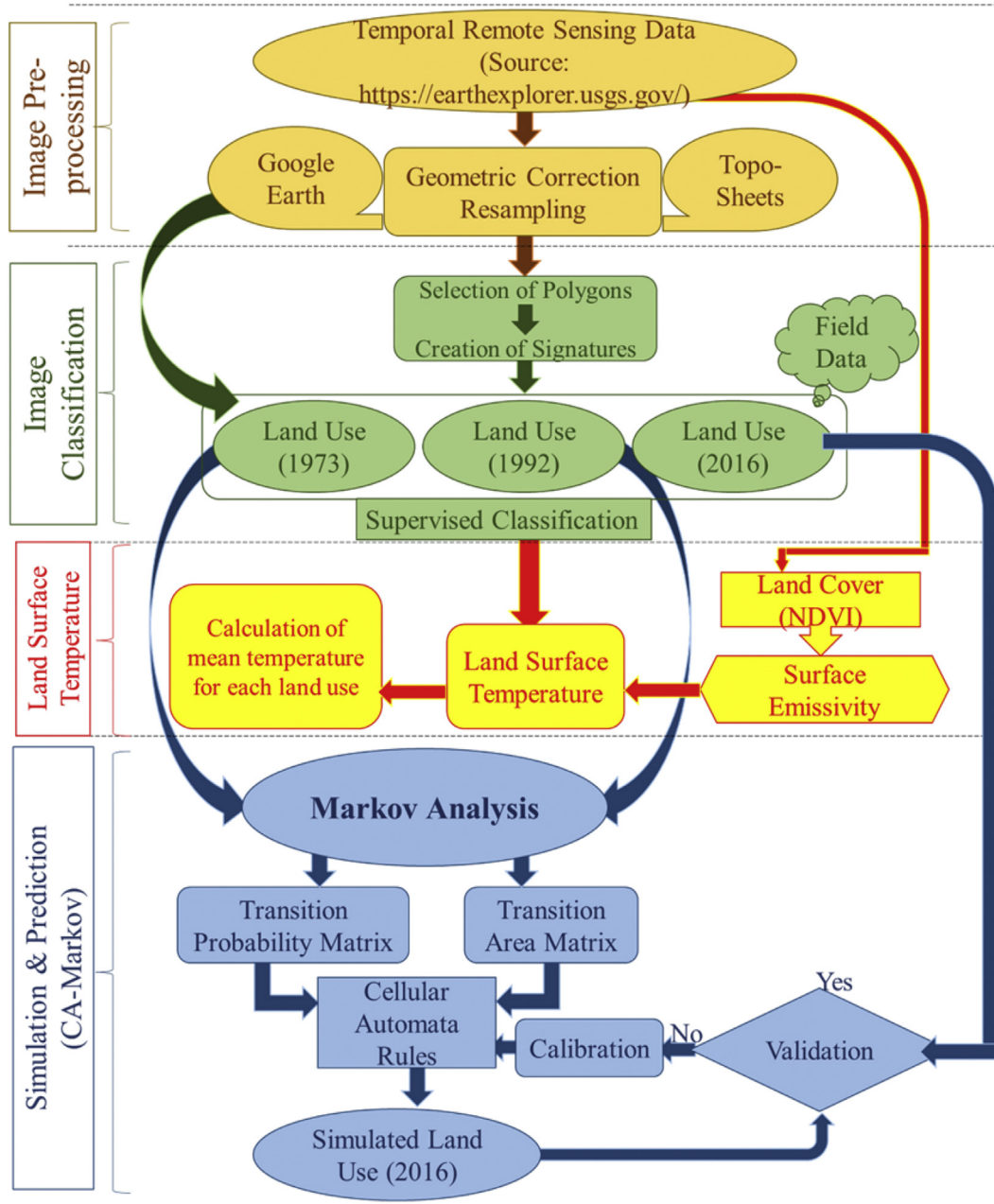


Fig. 3. Protocol for mapping, monitoring, modelling and visualization of LULC dynamics.

vegetation. Pre-calibrated GPS (Global Positioning System – Garmin GPS unit) used for field measurements. Land use analyses involved (i) generation of False Color Composite (FCC) of RS data (bands—green, red and NIR) (ii) selection of training polygons by covering 15% of the study area (polygons are uniformly distributed over the entire study area) (iii) loading these training polygons coordinates into pre-calibrated GPS, (vi) collection of the corresponding attribute data (training) from field, (iv) supplementing this information with Google Earth and (v) 60% of the training data has been used for supervised classification based on Gaussian maximum likelihood (GML) algorithm, while the balance is used for accuracy assessment. GRASS GIS (Geographical Resources Analysis Support System, <http://ces.iisc.ernet.in/grass>), a free and open source software is used for analysis.

LST is estimated pixel-wise across varied land use categories as per the standard protocol (Bharath et al., 2013) based on each land

use class emissivity that considers the amount of thermal infrared energy radiated from the Earth's surface of many different types of Earth surface processes, surface-atmosphere interactions. Estimation of LST using emissivity will provide more accurate estimation with appropriate calibration of atmospheric contamination by a separation of surface emissivity and temperature from radiance at ground level and atmospheric corrections (Li et al., 2013; Zásek and Oštr, 2012; Mohamed et al., 2017 Inamdar et al., 2008; Merlin et al., 2010). Emissivity is an intrinsic property of the surface, potential for enhancing ability to monitor landscape changes in environmentally sensitive zones as compared to other congruent practices (Hulley et al., 2014). The surface temperature of the area is calculated as per equation (3), through equations (1) and (2).

$$L_\lambda = M_L Q_{cal} + A_L \quad (1)$$

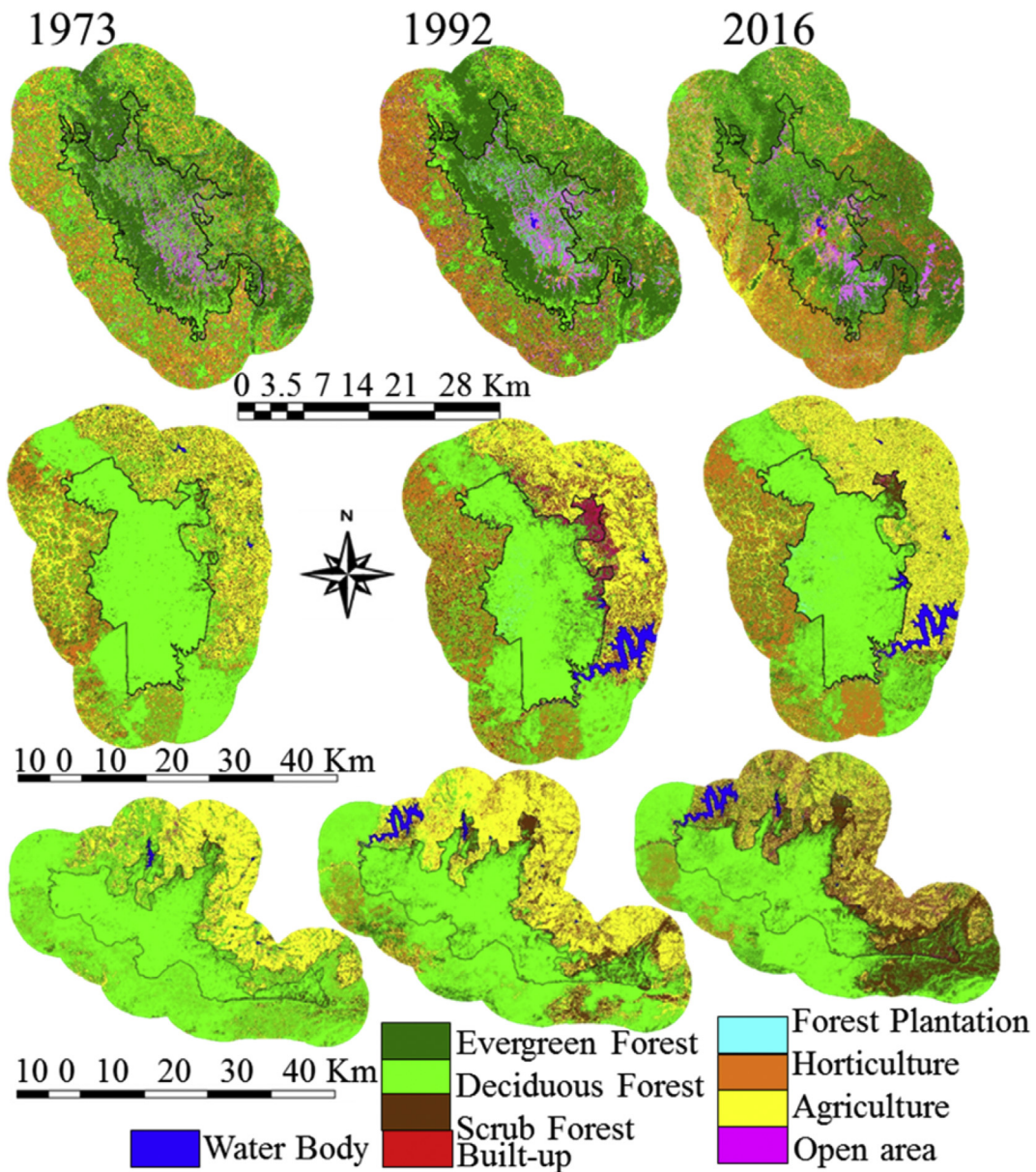


Fig. 4. (A–C): Temporal land use analysis for KNP, RTR, BTR from 1973 to 2016.

$$T_B = \left[\frac{K_2}{\ln\left(\frac{K_1}{L_\lambda} + 1\right)} \right] - 273 \quad (2)$$

L_λ represents the top of atmosphere spectral radiance (Watts/ $(m^2 \text{ srad } \mu\text{m})$). λ represents the wavelength of the thermal band. Q_{cal} is the DN value of the pixel under consideration. A_L and M_L are offset and gain factor respectively whose value for TM is $A_L = 1.238$, $M_L = 0.055$ and OLI is $A_L = 0.1$, $M_L = 3.3420 \times 10^{-4}$. K_1 (Watts/ $(m^2 \text{ srad } \mu\text{m})$) and K_2 (kelvin) represents the pre-launch calibration coefficients. Value of K_1 is 607.76 and K_2 is 1260.56 (for TM), while K_1 for OLI (Band 11) is 480.8883 and K_2 for is 1201.1442. T_B represents the At-satellite brightness temperature. Emissivity correction is carried out using surface emissivity for the specified LC derived from the methodology described in (Stathopoulou et al., 2007). The emissivity corrected land surface temperature (T_s) is computed from equation (3).

$$T_s = \frac{T_B}{1 + (\lambda \times T_B / \rho) \ln \epsilon} \quad (3)$$

where, λ is the wavelength of emitted radiance for which the peak response and the average of the limiting wavelengths ($\lambda = 11.5 \mu\text{m}$) were used, $\rho = h \times c / \sigma$ ($1.438 \times 10^{-2} \text{ mK}$), $\sigma = \text{Stefan Boltzmann's constant}$ ($5.67 \times 10^{-8} \text{ W m}^{-2} \text{ K}^{-4} = 1.38 \times 10^{-23} \text{ J/K}$), $h = \text{Planck's constant}$ ($6.626 \times 10^{-34} \text{ Jsec}$), $c = \text{velocity of light}$ ($2.998 \times 10^8 \text{ m/sec}$), and ϵ is spectral emissivity.

CA is used (Equation (4)) to obtain a spatial context and distribution map is based on Markov transitional probability and area by combining multi-criteria land allocations to predict land use changes. The neighborhood effect is incorporated through diamond filter of a kernel size of 5×5 pixels to create spatially explicit contiguous weighing factors (Bharath et al., 2014; Chen et al., 2013; Grinblat et al., 2016; Matthews et al., 2007; Pontius and Malanson, 2005). The temporal land use analyses provided spatial and

temporal aspects of LU changes and transition probability map and area matrix were generated based on Equations (5) and (6), Markov process. The original transition probability matrix (denoted by P) of land use type is obtained from two former land use maps (Grinblat et al., 2016; Matthews et al., 2007; Pontius and Malanson, 2005). CA coupled with Markov chain assisted in land use predictions of 2016 using the transitional probability and area matrix generated for 1973–1992. The validation has been carried out by evaluating with reference land use maps of 2016 (actual) using Kappa index for location and quantity. Based on these validations LU for 2025 was visualized considering intermediate iterations of 3-year time period. The CA model can be expressed as,

$$S(t, t+1) = F(S(t), N) \quad (4)$$

where, S is the set of discrete cellular states, N is the Cellular field, t and $t + 1$ indicate the different times, and F is the transformation function of cellular states in local space.

The Markov model is a theory based on the process of the formation of Markov random process systems for the prediction and optimal control theory method. Based on the Bayes conditional probability formula, the prediction of land use changes is calculated by the following equation:

$$P(N) = P(N-1)P_{ij} \quad (5)$$

where, $P_{(N)}$ is state probability of any times, and $P_{(N-1)}$ is

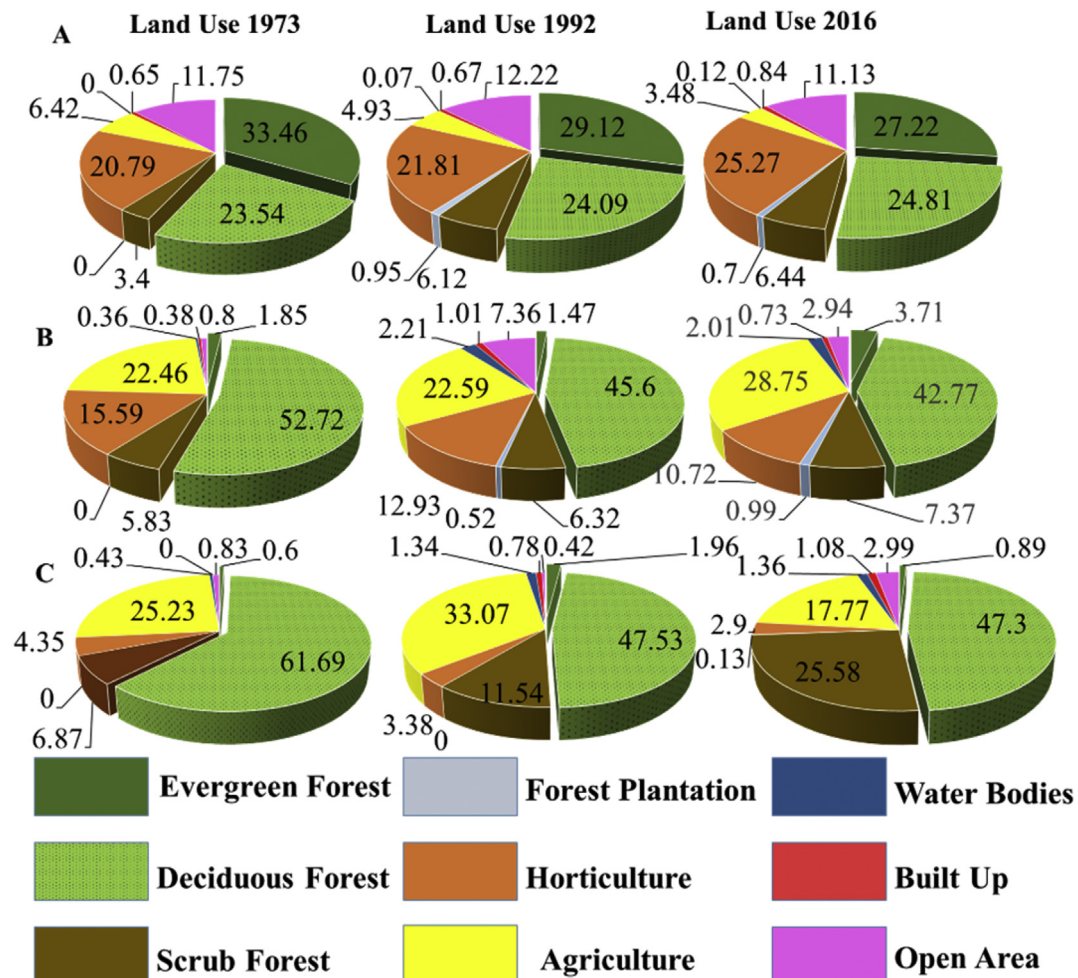


Fig. 5. (A–C): Variations in land use across three PAs for 1973, 1992 and 2016.

preliminary state probability.

Transition area matrix can be obtained by,

$$\text{Transition area Matrix } P = \begin{bmatrix} P_{11} & P_{12} & P_{13} \\ \vdots & \vdots & \vdots \\ P_{N1} & P_{N2} & P_{NN} \end{bmatrix} \quad (6)$$

where, P_{ij} is the sum of areas from the ith land use category to the jth category during the years from start point to target simulation periods, and n is the number of land use types. The transition area matrix must meet the following conditions

- i. $0 \leq P_{ij} \leq 1$
- ii. $\sum_{i,j=0}^n P_{ij} = 1$.

3. Results

3.1. Spatio temporal land use changes

KNP region has witnessed an increase in deciduous forest and scrub forest cover by 1.27% and 3.04% respectively at the cost of evergreen forest (reduction by 6.24%) during 1973–2016 (Fig. 4A). The increase in commercial plantation cover (4.48%) in buffer region and mining of iron ore (Kudremukh Iron Ore Company) are major agents of changes in the forest cover. Laka dam was constructed (for the operational purpose of mining industry- Kudremukh Iron Ore Company) which has further submerged some of the

Table 1

Transition probability matrix for KNP for 1992–2016.

	EF	DF	SF	FP	HO	AG	WB	BU	OA
Evergreen Forest	0.803	0.117	0.011	0.000	0.066	0.000	0.000	0.000	0.002
Deciduous Forest	0.000	0.619	0.065	0.011	0.236	0.015	0.000	0.006	0.049
Scrub Forest	0.000	0.059	0.546	0.014	0.048	0.058	0.000	0.011	0.264
Forest Plantation	0.000	0.045	0.246	0.535	0.000	0.000	0.006	0.000	0.168
Horticulture	0.000	0.205	0.014	0.005	0.611	0.119	0.000	0.014	0.032
Agriculture	0.000	0.048	0.034	0.001	0.046	0.611	0.000	0.013	0.248
Water Bodies	0.000	0.000	0.000	0.000	0.000	0.000	0.470	0.318	0.212
Built-Up	0.000	0.000	0.000	0.000	0.163	0.023	0.015	0.584	0.216
Open Area	0.000	0.001	0.156	0.120	0.022	0.142	0.006	0.014	0.539

forest area. RTR region has lost deciduous forest from 52.72% to 42.77% (1973–2016), with an increase in agriculture cover 6.29%, built-up area by 0.35% (Fig. 4B). The open area has increased by 2.14% due to increase in rampant grazing activities and over-exploitation of natural resources. Water bodies show an increase from 0.36% to 2.01% due to the construction of Taraka dam in 1984. BTR shows an increase of 18.71% scrub forest cover with a sharp decline of deciduous cover from 61.69 to 47.30% (Fig. 4C). The ever increasing human intervention in the form of tourism activities, plantations of teak, eucalyptus and frequent forest fires responsible for greater transition in this region. The human settlements in the buffer region contribute to 1.08% of the total region. Overgrazing has created more forest blanks (open spaces) in the core and also in the buffer region (increase in open areas by 2.16%), and these regions are infested with weeds such as *Parthenium hysterophorus* (Congress weed), *Chromolaena odorata* (Devil weed) affecting

native flora of BTR. Fig. 5 (A–C) provides the relative share of temporal land uses in KNP, RTR, BTR during four decades.

3.2. The role of LU changes on LST

Temperature and the mean temperature across the region was analyzed pixel-wise for 5 broad categories - (i) Vegetation includes evergreen forest, deciduous forest, scrub forest and forest plantations; (ii) Agriculture includes horticulture and agriculture; (iii) water bodies (lakes, streams, rivers); (iv) Built-up and (v) Open area (fallow land), by reclassifying earlier 9 land use categories (Figs. 4 and 5). Thermal signatures of different LU types in the study area helped in understanding the role of respective LU category to heat phenomenon. In KNP, the average temperature across the National Park has increased by around 4° C due to the loss of evergreen forest which has allowed the soil beneath the canopy to get

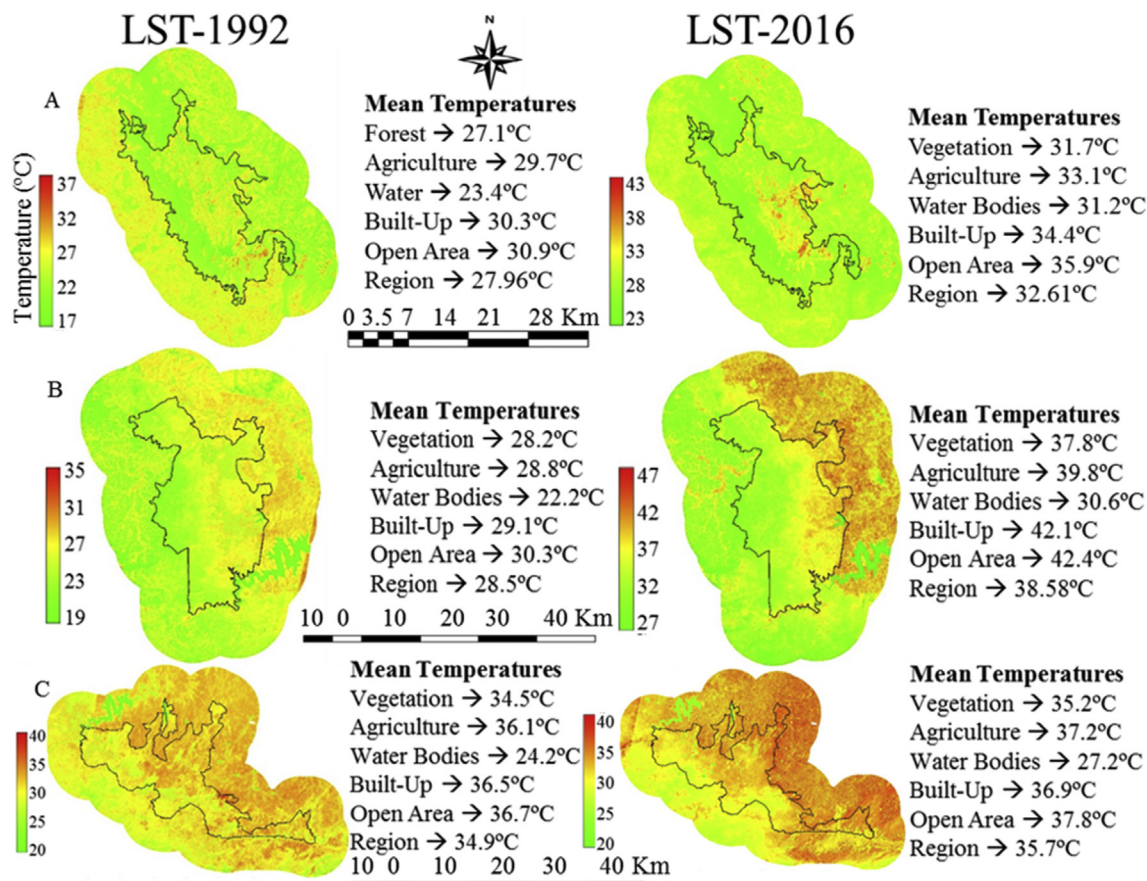


Fig. 6. (A–C): Temporal pixel level LST across PAs.

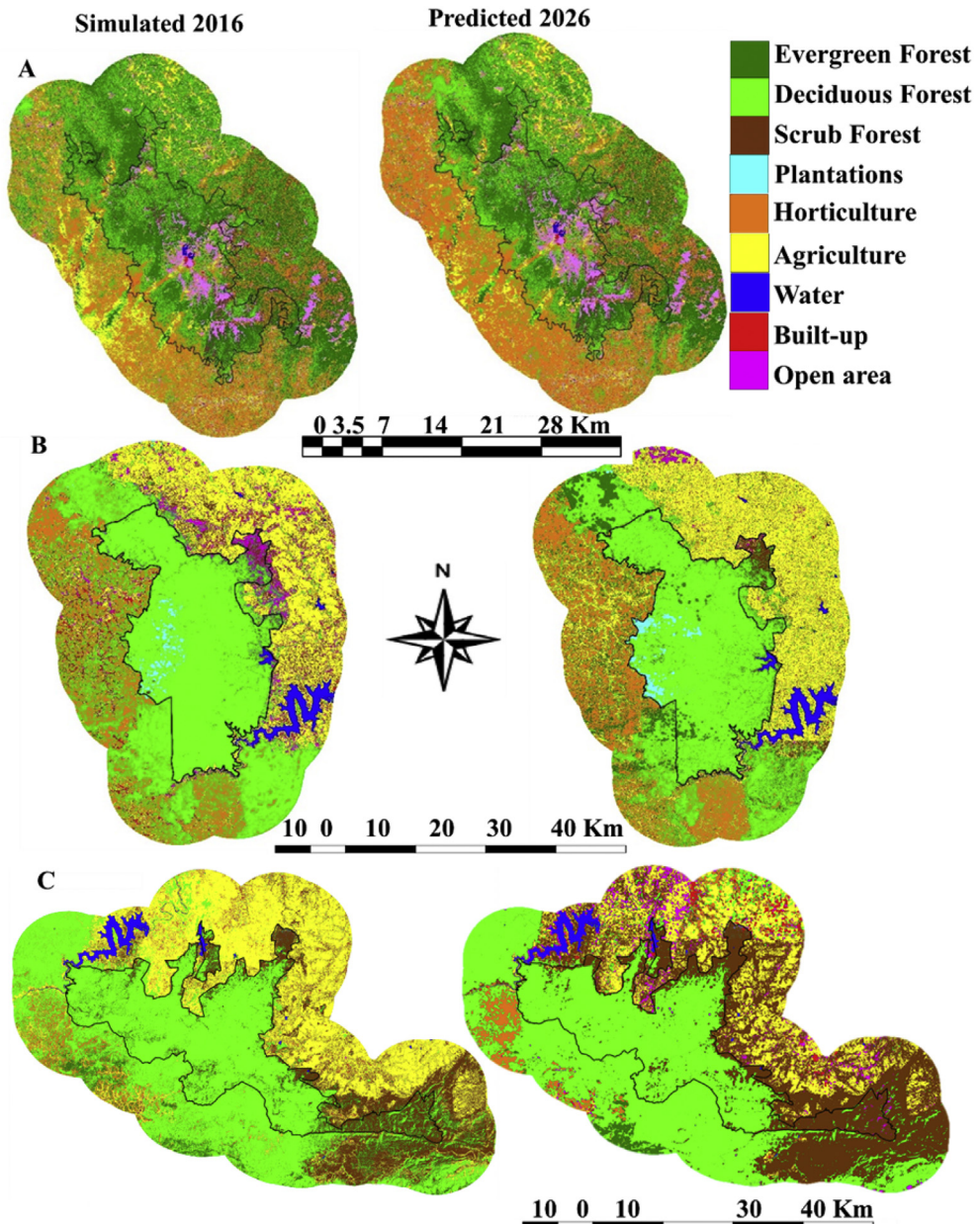


Fig. 7. (A–C): Simulated and predicted land uses in PAs.

exposed to sunlight and absorb more heat, leading to a rise in mean temperature. The dam has a lot of deposits of dumped iron ore waste which has led to the rise in temperature of the water body as well. The mean vegetation temperature is increased by around 9°C in RTR due to removal of native forest and increase in teak, eucalyptus plantations, which exposes the ground to direct sunlight. This region contributes to a highest change in temperature among the study area. BTR shows that there is an increase of around 1°C in the region during the 1992–2016 due to transition of forest cover. RTR and BTR areas are infested by various non-native species which has led to a reduction in water retaining capability of the soil with rise in temperature. There were incidences of forest fire (natural and man-made), due to which the surface gets exposed and heats up more which further increases the temperature. The increase in temperature has also enhanced the chances of forest fire again, as it is a cyclic process (Vlassova et al., 2014). The intensified LULC

changes induces prolonged drought, which can trigger large-scale landscape changes through vegetation mortality due to water stress (Fensham and Holman, 1999; Ruthrof et al., 2016), loss of productivity (Cooper et al., 2017) and land surface conditions for decades (Breshears et al., 2005; Kulakowski et al., 2011).

3.3. Modelling and visualization of land use

Modelling and visualization of LU dynamics in 3 PAs were analyzed using CA-Markov and validation was done through Kappa statistics. Transition probability matrices were generated for PAs as shown in Table 1, simulated and current land use maps were validated. Fig. 6 shows the simulated 2016 and predicted land uses for 2026. Table 2 shows the percentage of various land use categories. Modelling LU in KNP region shows evergreen forest will continue to degrade and will cover only 23.04% by 2026. The same trend

Table 2

Simulated and predicted Land use details of PAs for 2016 & 2026.

Category	KNP		RTR		BTR	
	Simulated 2016	Predicted 2026	Simulated 2016	Predicted 2026	Simulated 2016	Predicted 2026
Evergreen Forest	28.53	23.04	1.19	5.32	1.95	1.06
Deciduous Forest	20.05	18.95	47.01	40.16	43.58	44.09
Scrub Forest	5.06	5.69	6.58	7.16	17.72	31.00
Forest Plantation	0.41	0.48	0.94	1.15	0.13	0.13
Horticulture	29.83	36.16	13.21	17.16	3.35	3.32
Agriculture	7.27	5.62	21.85	25.13	30.73	14.62
Water Bodies	0.13	0.13	2.00	1.98	1.37	1.38
Built-Up	0.66	0.99	1.39	0.98	0.75	1.21
Open Area	8.06	8.93	5.84	0.96	0.40	3.21
Total	100	100	100	100	100	100
KAPPA	0.74	0.81			0.75	

continues for deciduous with loss of 6%. Commercial plantations in the region will increase tremendously and will cover almost 1/3rd of the total region. Deciduous forest will cover 40.16% with increases in scrub forest cover by 2026 in RTR region. Agricultural and Horticultural activities are predicted to remain same. Evergreen forests show a slight increase as it is present on the hill tops, thus making it difficult for humans to intervene. BTR region also would experience the degradation of forests with 3.21% reduction in deciduous cover by 2026. Scrub forest will be the second land use after deciduous forest to dominate the region and would cover 31%. All these regions depict an increase in built-up area and horticulture, which signifies increased human interventions, and the continued forest vegetation degradation. This will have a cascading impact with increments in temperature, disturbing the biodiversity, species regeneration, etc. and may lead to vegetation die-off. It will be difficult for the sustenance of native cover in changed environment leading to an extinction of endemic species. Implementation of conservation norms with rigid protection measures, enrichment of degraded forest patches with the native vegetation, enriching the Gomala Lands (grass lands) are necessary to sustain natural resources in PAs. The government needs to take appropriate mitigation measures in the animal movement paths by (i) creating water bodies, (ii) growing fodder crops, (iii) restrictions of inappropriate crops and (iv) eviction of an unauthorized occupation of forest lands. Human interferences are evident either through diversions of natural drains or senseless commercial crops, which have further complicated the conservation of endangered fauna (see Fig. 7).

4. Conclusion

PAs are characterized by high levels of biodiversity and endemism. LULC changes are perceived as a major agent of landscape transitions in PAs. Mapping, monitoring and modelling will help in framing appropriate management policies to preserve ecosystem functions and resilience. All studied regions depict an increase in built-up area and horticulture that signifies increment in human interventions. KNP show loss of evergreen cover from 33 to 27% by 2016 and higher loss is witnessed in RTR region's deciduous cover. LU changes have altered ecological functions of PAs such as microclimatic moderation evident from the enhanced LST with time. The impacts in these ecologically fragile regions are long-term and non-reversible. The increase in temperature is observed in RTR, KNP signifies there will be more adverse effects in near future. The modelling prediction for 2026 reveals the loss of evergreen cover in KNP (27–18%), deciduous cover in RTR (42–40%) followed by BTR (47–44%) due to increasing in horticulture and grazing activities. The results of this study would help local authorities to understand

the current situation and visualize the possible future conditions to adopt appropriate conservation strategies for management of PAs. The management plans are to be prepared to mitigate anthropogenic impacts in PAs and to address human-animal conflicts through ecosystem-based management approaches including awareness programs (outreach) in the core and buffer zones.

Acknowledgement

We are grateful to (i) Karnataka Accounts and Audit General, Government of Karnataka (R1011), (ii) the Natural Resources Data Management System (NRDMS) Division, Ministry of Science and Technology (CES/TVR/DST/1045), (iii) the Ministry of Environment Forest and Climate Change, Government of India (DE007) and (iv) Indian Institute of Science (CES/TVR/KAAG_GOK/01) for the financial and the sustained infrastructure support.

References

- Allen, C.D., Breshears, D.D., McDowell, N.G., 2015. On underestimation of global vulnerability to tree mortality and forest die-off from hotter drought in the Anthropocene. *Ecosphere* 6, art129. <http://dx.doi.org/10.1890/ES15-00203.1>.
- Bagley, J.E., Desai, A.R., Harding, K.J., Snyder, P.K., Foley, J.A., 2014. Drought and deforestation: has land cover change influenced recent precipitation extremes in the Amazon? *J. Clim.* 27, 345–361. <http://dx.doi.org/10.1175/JCLI-D-12-00369.1>.
- Batty, M., Torrens, P.M., 2005. Modelling and prediction in a complex world. *Futures* 37, 745–766. <http://dx.doi.org/10.1016/j.futures.2004.11.003>.
- Bharath, S., Rajan, K.S., Ramachandra, T.V., 2013. Land surface temperature response to land use land cover dynamics. *Geoinform. Geostat. Overv.* 1 <http://dx.doi.org/10.4172/2327-4581.100112>.
- Bharath, S., Rajan, K.S., Ramachandra, T.V., 2014. Status and future transition of rapid urbanizing landscape in central Western Ghats - CA based approach. *ISPRS Ann. Photogramm. Remote Sens. Spat. Inf. Sci.* 2, 69–75. <http://dx.doi.org/10.5194/isprsaannals-II-8-69-2014>.
- Breshears, D.D., Cobb, N.S., Rich, P.M., Price, K.P., Allen, C.D., Balice, R.G., Romme, W.H., Kastens, J.H., Floyd, M.L., Belnap, J., Anderson, J.J., Myers, O.B., Meyer, C.W., 2005. Regional vegetation die-off in response to global-change-type drought. *Proc. Natl. Acad. Sci.* 102, 15144–15148. <http://dx.doi.org/10.1073/pnas.0505734102>.
- Chase, T.N., Pielke Sr., R. a., Kittel, T.G.F., Nemani, R.R., Running, S.W., 2000. Simulated impacts of historical land cover changes on global climate in northern winter. *Clim. Dyn.* 16, 93–105. <http://dx.doi.org/10.1007/s003820050007>.
- Chen, C.F., Son, N.T., Chang, N.B., Chen, C.R., Chang, L.Y., Valdez, M., Centeno, G., Thompson, C.A., Aceituno, J.L., 2013. Multi-decadal mangrove forest change detection and prediction in Honduras, central America, with landsat imagery and a markov chain model. *Remote Sens.* 5, 6408–6426. <http://dx.doi.org/10.3390/rs5126408>.
- Cooper, L.A., Ballantyne, A.P., Holden, Z.A., Landguth, E.L., 2017. Disturbance impacts on land surface temperature and gross primary productivity in the western United States. *J. Geophys. Res. Biogeosci.* 122, 930–946. <http://dx.doi.org/10.1002/2016JG003622>.
- D'Odorico, P., He, Y., Collins, S., De Wekker, S.F.J., Engel, V., Fuentes, J.D., 2013. Vegetation-microclimate feedbacks in woodland-grassland ecotones. *Glob. Ecol. Biogeogr.* 22, 364–379. <http://dx.doi.org/10.1111/geb.12000>.
- de Groot, R., Brander, L., van der Ploeg, S., Costanza, R., Bernard, F., Braat, L., Christie, M., Crossman, N., Ghermandi, A., Hein, L., Hussain, S., Kumar, P.,

McVittie, A., Portela, R., Rodriguez, L.C., ten Brink, P., van Beukering, P., 2012. Global estimates of the value of ecosystems and their services in monetary units. *Ecosyst. Serv.* 1, 50–61. <http://dx.doi.org/10.1016/j.ecoser.2012.07.005>.

Fensham, R.J., Holman, J.E., 1999. Temporal and spatial patterns in drought-related tree dieback in Australian savanna. *J. Appl. Ecol.* 36, 1035–1050. <http://dx.doi.org/10.1046/j.1365-2664.1999.00460.x>.

Fischer, J., Lindenmayer, D.B., 2007. Landscape modification and habitat fragmentation: a synthesis. *Glob. Ecol. Biogeogr.* <http://dx.doi.org/10.1111/j.1466-8238.2007.00287.x>.

Gaston, K.J., Jackson, S.F., Nagy, A., Cantú-Salazar, L., Johnson, M., 2008. Protected areas in Europe: principle and practice. *Ann. N. Y. Acad. Sci.* <http://dx.doi.org/10.1196/annals.1439.006>.

Grinblat, Y., Gilichinsky, M., Benenson, I., 2016. Cellular automata modeling of land-use/land-cover dynamics: questioning the reliability of data sources and classification methods. *Ann. Am. Assoc. Geogr.* 106, 1299–1320. <http://dx.doi.org/10.1080/24694452.2016.1213154>.

Halder, S., Saha, S.K., Dirmeyer, P.A., Chase, T.N., Goswami, B.N., 2016. Investigating the impact of land-use land-cover change on Indian summer monsoon daily rainfall and temperature during 1951–2005 using a regional climate model. *Hydrol. Earth Syst. Sci.* 20, 1765–1784. <http://dx.doi.org/10.5194/hess-20-1765-2016>.

Hamilton, C.M., Martinuzzi, S., Plantinga, A.J., Radeloff, V.C., Lewis, D.J., Thogmartin, W.E., Heglund, P.J., Pidgeon, A.M., 2013. Current and future land use around a nationwide protected area network. *PLoS One* 8, 31. <http://dx.doi.org/10.1371/journal.pone.0055737>.

Hansen, A.J., DeFries, R.S., Turner, W., 2004. Land use change and biodiversity. In: Gutman, G., Janetos, A.C., Justice, C.O., Moran, E.F., Mustard, J.F., Rindfuss, R.R., Skole, D., Turner, B.L., Cochrane, M.A. (Eds.), *Land Change Science: Observing, Monitoring and Understanding Trajectories of Change on the Earth's Surface*. Springer Netherlands, Dordrecht, pp. 277–299. http://dx.doi.org/10.1007/978-1-4020-2562-4_16.

Hulley, G., Veraverbeke, S., Hook, S., 2014. Thermal-based techniques for land cover change detection using a new dynamic MODIS multispectral emissivity product (MOD21). *Remote Sens. Environ.* 140, 755–765. <http://dx.doi.org/10.1016/j.rse.2013.10.014>.

Inamdar, A.K., French, A., Hook, S., Vaughan, G., Luckett, W., 2008. Land surface temperature retrieval at high spatial and temporal resolutions over the southwestern United States. *J. Geophys. Res. Atmos.* 113 <http://dx.doi.org/10.1029/2007JD009048>.

Kintz, D., Young, K., Crews-Meyer, K., 2006. Implications of land use/land cover change in the buffer zone of a national park in the tropical Andes. *Environ. Manag.* 38, 238–252. <http://dx.doi.org/10.1007/s00267-005-0147-9>.

Krieger, D., 2001. Economic Value of Forest Ecosystem Services : a Review [WWW Document]. *Wilderness Soc.* http://www.cfr.washington.edu/classes.esrm.465/2007/readings/ws_valuation.pdf.

Kulakowski, D., Bebi, P., Rixen, C., 2011. The interacting effects of land use change, climate change and suppression of natural disturbances on landscape forest structure in the Swiss Alps. *Oikos* 120, 216–225. <http://dx.doi.org/10.1111/j.1600-0706.2010.18726.x>.

Lambin, E.F., Meyfroidt, P., 2011. Global land use change, economic globalization, and the looming land scarcity. *Proc. Natl. Acad. Sci. U. S. A.* 108, 3465–3472. <http://dx.doi.org/10.1073/pnas.1100480108>.

Le Quéré, C., Peters, G.P., Andres, R.J., Andrew, R.M., et al., 2013. Global carbon budget 2013. *Earth Syst. Sci. Data Discuss.* 6, 689–760. <http://dx.doi.org/10.5194/essd-6-689-2013>.

Li, Z.L., Wu, H., Wang, N., Qiu, S., Sobrino, J.A., Wan, Z., Tang, B.-H., Yan, G., 2013. Land surface emissivity retrieval from satellite data. *Int. J. Remote Sens.* 34, 3084–3127. <http://dx.doi.org/10.1080/01431161.2012.716540>.

Li, Y., Zhao, M., Mildrexler, D.J., Motesharrei, S., Mu, Q., Kalnay, E., Zhao, F., Li, S., Wang, K., 2016. Potential and Actual impacts of deforestation and afforestation on land surface temperature. *J. Geophys. Res. Atmos.* 121, 14,314–372,386. <http://dx.doi.org/10.1002/2016JD024969>.

Mallick, J., Kant, Y., Bharath, B.D., 2008. Estimation of land surface temperature over Delhi using Landsat-7 ETM+. *J. Ind. Geophys. Union* 12, 131–140.

Matthews, R.B., Gilbert, N.G., Roach, A., Polhill, J.G., Gotts, N.M., 2007. Agent-based land-use models: a review of applications. *Landsc. Ecol.* <http://dx.doi.org/10.1007/s10980-007-9135-1>.

Merlin, O., Duchemin, B., Hagolle, O., Jacob, F., Coudert, B., Chehbouni, G., Dedieu, G., Garatza, J., Kerr, Y., 2010. Disaggregation of MODIS surface temperature over an agricultural area using a time series of Formosat-2 images. *Remote Sens. Environ.* 114, 2500–2512. <http://dx.doi.org/10.1016/j.rse.2010.05.025>.

Mohamed, A.A., Odindi, J., Mutanga, O., 2017. Land surface temperature and emissivity estimation for Urban Heat Island assessment using medium- and low-resolution space-borne sensors: a review. *Geocarto Int.* 32, 455–470. <http://dx.doi.org/10.1080/10106049.2016.1155657>.

Mondal, M.S., Sharma, N., Garg, P.K., Kappas, M., 2016. Statistical independence test and validation of CA Markov land use land cover (LULC) prediction results. *Egypt. J. Remote Sens. Sp. Sci.* 19, 259–272. <http://dx.doi.org/10.1016/j.ejrs.2016.08.001>.

Pal, S., Ziaul, S., 2016. Detection of land use and land cover change and land surface temperature in English Bazar urban centre. *Egypt. J. Remote Sens. Sp. Sci.* <http://dx.doi.org/10.1016/j.ejrs.2016.11.003>.

Pontius, G.R., Malanson, J., 2005. Comparison of the structure and accuracy of two land change models. *Int. J. Geogr. Inf. Sci.* 19, 243–265. <http://dx.doi.org/10.1080/13658810410001713434>.

Ramachandra, T.V., 2014. Hydrological responses at regional scale to landscape dynamics. *J. Biodivers.* 5, 11–32.

Ramachandra, T.V., Bharath, S., Bharath, H.A., 2014. Spatio-temporal dynamics along the terrain gradient of diverse landscape. *J. Environ. Eng. Landsc. Manag.* 22, 50–63. <http://dx.doi.org/10.3846/16486897.2013.808639>.

Ramachandra, T.V., Bharath, S., Chandran, M.D.S., 2016a. Geospatial analysis of forest fragmentation in Uttara Kannada district, India. *For. Ecosyst.* 3, 10. <http://dx.doi.org/10.1186/s40663-016-0069-4>.

Ramachandra, T.V., Bharath, S., Rajan, K.S., Chandran, M.D.S., 2016b. Stimulus of developmental projects to landscape dynamics in Uttara Kannada, central Western Ghats. *Egypt. J. Remote Sens. Sp. Sci.* 19, 175–193. <http://dx.doi.org/10.1016/j.ejrs.2016.09.001>.

Ruthrof, K.X., Fontaine, J.B., Matusick, G., Breshears, D.D., Law, D.J., Powell, S., Hardy, G., 2016. How drought-induced forest die-off alters microclimate and increases fuel loadings and fire potentials. *Int. J. Wildl. Fire* 25, 819–830. <http://dx.doi.org/10.1071/WF15028>.

Sanderson, E.W., Jaiteh, M., Levy, M.A., Redford, K.H., Wannebo, A.V., Woolmer, G., 2002. The Human Footprint and the Last of the wild the human footprint is a global map of human influence on the land surface, which suggests that human beings are stewards of nature, whether we like it or not. *Bioscience* 52, 891–904.

Stathopoulou, M., Cartalis, C., Petrakis, M., 2007. Integrating Corine Land Cover data and Landsat TM for surface emissivity definition: application to the urban area of Athens, Greece. *Int. J. Remote Sens.* 28, 3291–3304. <http://dx.doi.org/10.1080/01431160600993421>.

Val Martin, M., Heald, C.L., Lamarque, J.F., Tilmes, S., Emmons, L.K., Schichtel, B.A., 2015. How emissions, climate, and land use change will impact mid-century air quality over the United States: a focus on effects at national parks. *Atmos. Chem. Phys.* 15, 2805–2823. <http://dx.doi.org/10.5194/acp-15-2805-2015>.

Verburg, P.H., Schot, P.P., Dijst, M.J., Veldkamp, A.T., 2004. Land use change modelling: current practice and research priorities. *GeoJournal* 61, 309–324. <http://dx.doi.org/10.1007/s10708-004-4946-y>.

Vinay, S., Bharath, S., Bharath, H.A., Ramachandra, T.V., 2013. Hydrologic model with landscape dynamics for drought monitoring. In: *Joint International Workshop of ISPRS VIII/1 and WG IV/4 on Geospatial Data for Disaster and Risk Reduction*. Hyderabad.

Vlassova, L., Pérez-Cabello, F., Mimbrero, M.R., Llovería, R.M., García Martín, A., 2014. Analysis of the relationship between land surface temperature and wildfire severity in a series of landsat images. *Remote Sens.* 6, 6136–6162. <http://dx.doi.org/10.3390/rs6076136>.

Zakšek, K., Oštir, K., 2012. Downscaling land surface temperature for urban heat island diurnal cycle analysis. *Remote Sens. Environ.* 117, 114–124. <http://dx.doi.org/10.1016/j.rse.2011.05.027>.